Science & Technology Facilities Council

Technical Report
RAL-TR-2016-009

Understanding the motion of a long bar under electric pulse heating; stress, strain and strain rate

JRJ Bennett

July 2016

Enquiries concerning this report should be addressed to:

RAL Library
STFC Rutherford Appleton Laboratory
Harwell Oxford
Didcot
OX11 0QX

Tel: +44(0)1235 445384
Fax: +44(0)1235 446403
email: libraryral@stfc.ac.uk

Science and Technology Facilities Council reports are available online at: http://epubs.stfc.ac.uk

ISSN 1358-6254

UKNF/Target/N2/2011
16 March 2011

Understanding the Motion of a Long Bar under Electric Pulse Heating; Stress, Strain and Strain Rate

J. R. J. Bennett

Rutherford Appleton Laboratory, Chilton, Didcot, Oxon. OX11 0QX

Understanding the Motion of a Long Bar under Electric Pulse Heating;

Stress, Strain and Strain Rate

1. Introduction

Consider a long straight circular section unconstrained bar freely suspended from its centre. A pulsed current is passed along the length of the bar. The bar expands due to the temperature rise. Under certain conditions the bar suffers a thermal shock which excites natural resonance vibrations both longitudinally and radially. The electric current also produces a magnetic field, which induces forces on the bar. This note tries to explain the stresses and motions of the bar under various conditions and compares them to the observed motions.

When a body is struck a sharp blow a wave is transmitted along the body with a velocity,

$$c = \sqrt{\frac{E}{\rho}} \tag{1}$$

where E is Young's modulus of elasticity and ρ is the density [1,2]. (Depending on the type of wave generated the velocity is moderated by terms involving Poisson's ratio [1,2].) If the blow is very gentle and gradual, the body acts quasi-statically and then there is no wave, just a deformation. Very approximately, if an impulse is given to the body over a period of time, τ, much greater than the time taken for a wave to cross the dimension, D of the body,

$\tau >> D/c$

then the motion is quasi-static. When the impulse is given over a period,

$\tau << D/c$

then the body is excited into its natural modes of resonance. In many cases with finite rise times, both of these extremes will occur simultaneously. It is interesting to consider the case of the long thin bar of length $2L$ and radius a. The period, τ, in the radial direction is $\tau_r = a/c$ while in the axial is $\tau_z = L/c$. With $a << L$ it is quite possible that the motion can be treated quasi-statically in the radial and dynamically as a wave motion in the axial.

Bargmann [3] gives a good analysis of the stress and motion of a bar bombarded by a fast proton beam pulse, as does Sievers [4]. The analyses include both very short pulses (instantaneous) and intermediate pulses.

2. Axial Stress, Strain and Motion with an Instantaneous (very short) Pulse

2.1 Qualitative Considerations

Consider a circular section bar freely suspended from its centre, of radius a and length $2L$, where $L >> a$, (see Figure 1).

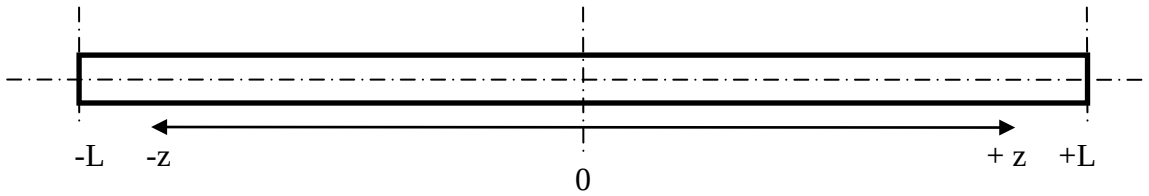

Figure 1. A freely suspended bar of length $2L$.

The bar is instantaneously and uniformly raised in temperature by ΔT at time $t = 0$. The bar consequently expands radially by, r, and longitudinally by $2l$, given by, $r = \alpha a \Delta T$, $l = \alpha L \Delta T$, where α is the coefficient of linear expansion. Because of the inertia of the bar, the expansion takes time to accomplish. Initially, the whole bar is under a uniform compressional stress, $\sigma = El/L$, where E is Young's modulus of elasticity. There are no external forces on the bar and the centre of gravity does not move. Since the external surfaces of the bar are free, the stresses at the surfaces are always zero. For a long thin bar, where a/L is small and coupling of the motions between the radial and longitudinal can be ignored, the axial stress can be calculated as a one dimensional problem. The resulting axial stress, σ, in the bar is given approximately by the following equations for a long thin elastic bar [1-4],

$$\frac{\partial^2 \sigma}{\partial z^2} = \frac{1}{c^2}\frac{\partial^2 \sigma}{\partial t^2} \tag{2}$$

At a point z along the axis from the centre of the bar the longitudinal stress at time t is,

$$\sigma_l(z,t) = E\alpha\Delta T \frac{4}{\pi}\sum_{n=0}^{\infty}\frac{(-1)^n}{(2n+1)}\left\{\cos\left[\frac{(2n+1)\pi}{2L}z\right]\cos\left[\frac{(2n+1)\pi}{2L}ct\right]\right\} \tag{3}$$

Equation (3) produces a square stress distribution. It may be re-expressed as the sum of two terms representing identical square waves travelling in opposite directions at velocity c,

$$\sigma_l(z,t) = E\alpha\Delta T \frac{2}{\pi}\sum_{n=0}^{\infty}\frac{(-1)^n}{(2n+1)}\left\{\cos\left[\frac{(2n+1)\pi}{2L}(z+ct)\right] + \cos\left[\frac{(2n+1)\pi}{2L}(z-ct)\right]\right\} \tag{4}$$

where n is an integer and the compressional wave velocity [1-4] is (as equation 1),

$$c^2 = \frac{E}{\rho} \tag{5}$$

Figure 2 shows the stress distribution along the bar at different times. The corresponding stresses versus time plots at various positions along the length of the bar are shown in Figure 3. All times, $t*$, are given in units of L/c. Damping of the stress waves is ignored in the calculations; in reality there is damping and the amplitude of the stresses and subsequent motions reduce with time.

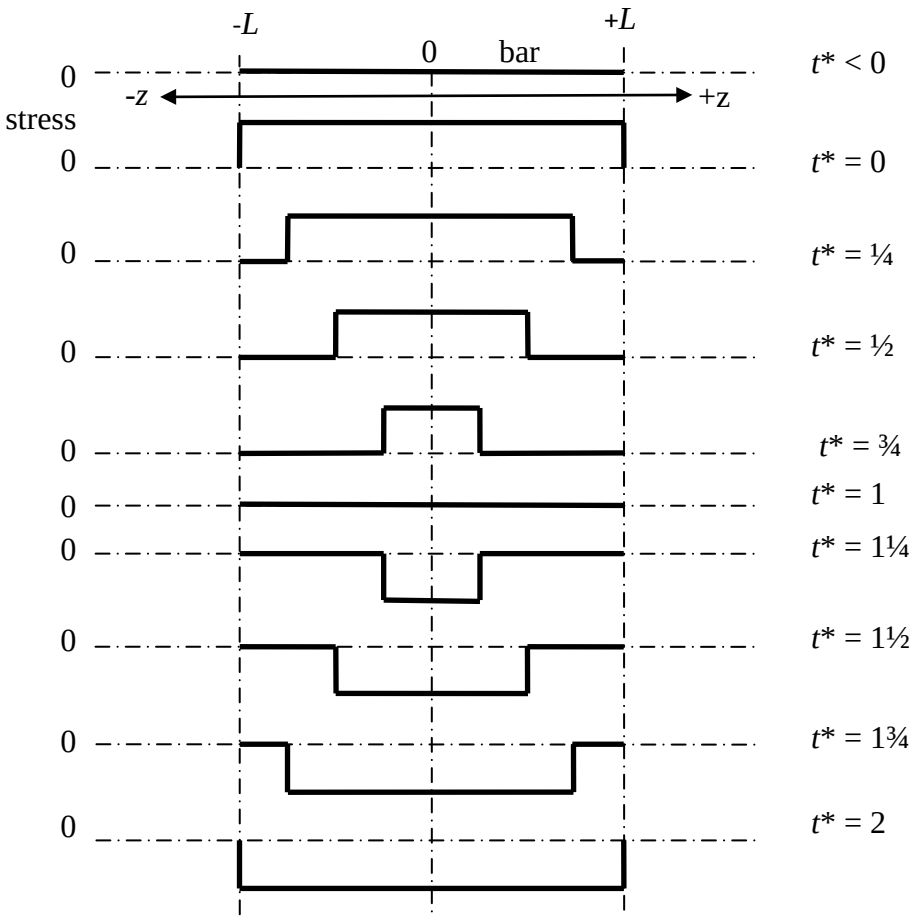

Figure 2. The stress along the length of the bar at different times, t^*, in units of L/c. The stresses reverse every period of time, $t^* = 2$.

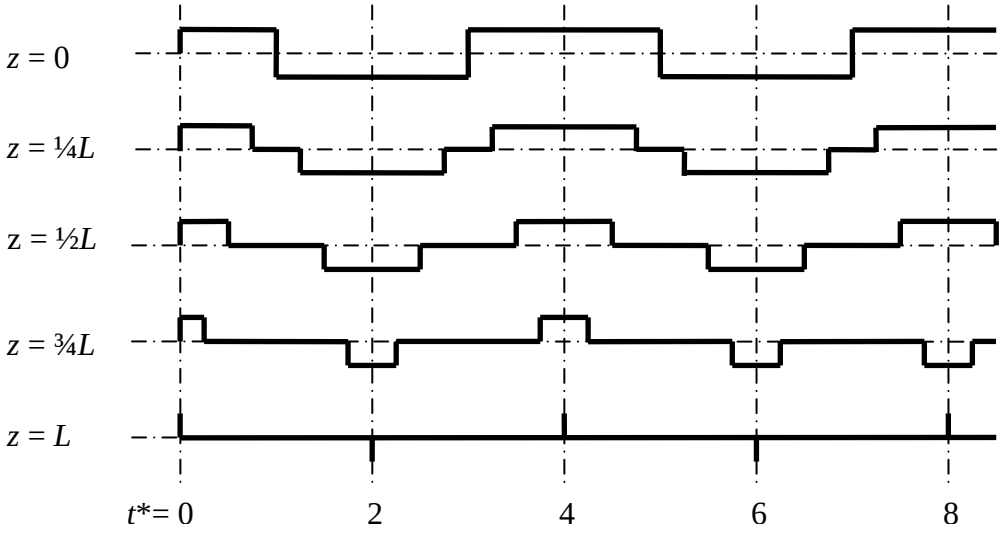

Figure 3. Stress pulses experienced at different positions along the bar as a function of t^*.

At $t = 0$, the relaxation wave starts to travel down the bar from the ends; the velocity at the ends of the bar instantly increases to a constant value, V_0. The end of the bar expands to its natural size at the new temperature at $t^* = 1$ when the stress is zero throughout the length of the bar. At $t^* = 2$ the ends receive an impulse in the reverse direction and the velocity

decreases stepwise to $-V_0$. At $t^* = 4$ the end slice receives another impulse increasing the velocity again. This continues, as shown in Figure 4. The displacement of the ends under constantly reversing velocities is also shown in Figure 4. Notice that the average displacement (the "new size" line) corresponds to the size of the bar at the new temperature and the amplitude of the excursion is equal to the thermal expansion.

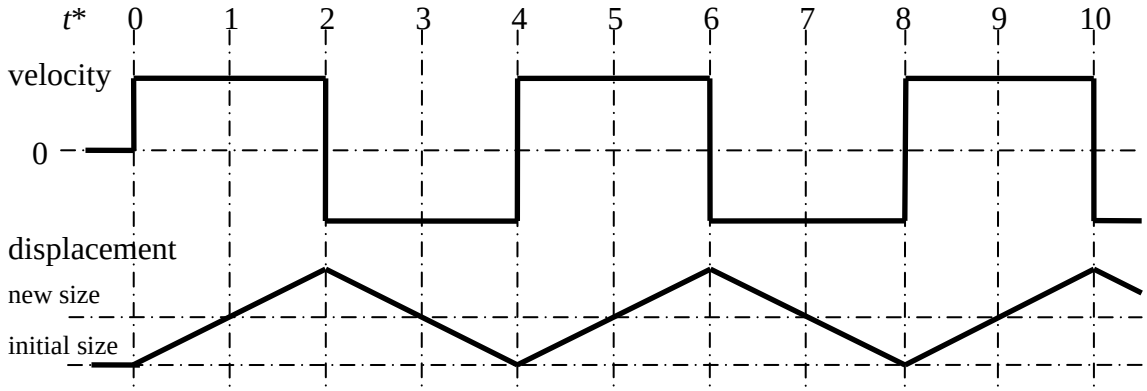

Figure 4. Velocity and displacement at the end of the bar as a function of time, t^*.

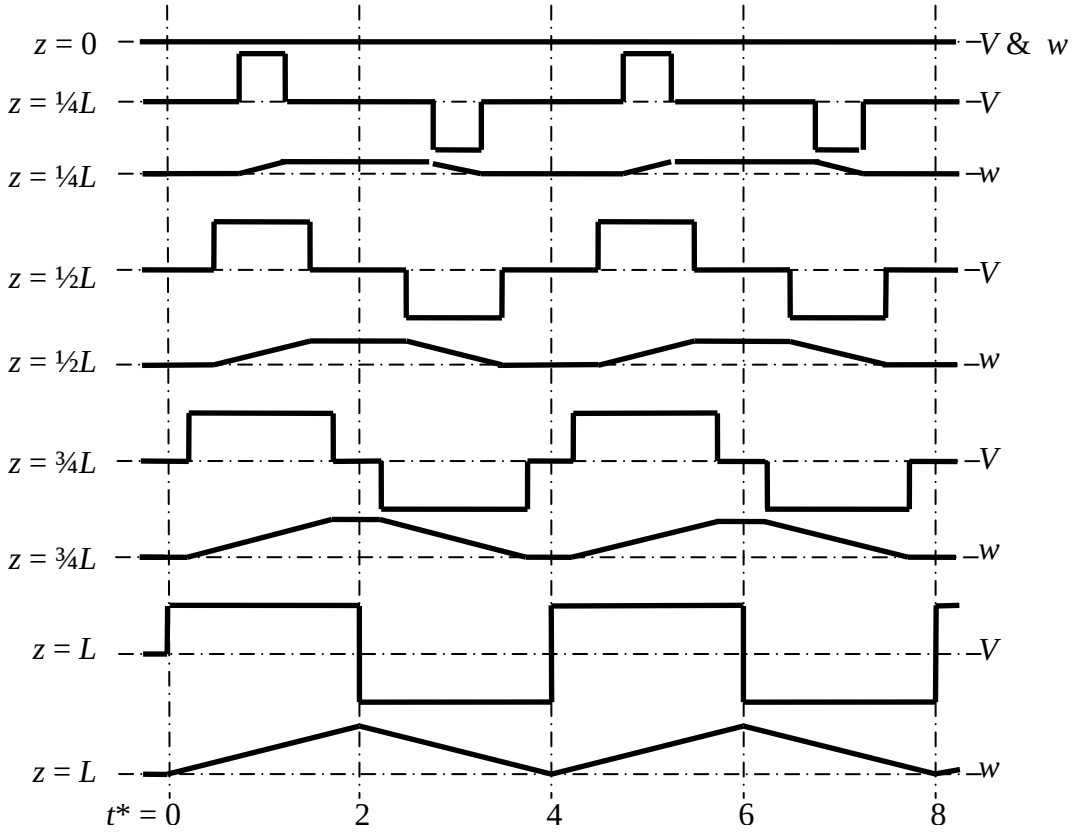

Figure 5. Velocity, V, and displacement, w, as a function of time, t^*, at various values of z.

Now consider the motion at different positions along the length of the bar. The longitudinal velocity, V, and displacement, w, versus t^* is shown in Figure 5, for different values of z.

At first sight the motion and the stress plots, Figures 5 and 3, do not seem to agree. One would expect the motion to occur when there is stress on the bar and not when the stress is zero. However, the stress originally arises from the fact that the bar is prevented from expanding from its original size by the inertia of the bar. The inertial force is equal to the elastic force resulting in zero expansion. Only when the relaxation wave passes and the stress go to zero can the bar move.

2.2 Mathematical expressions for the longitudinal motion of the bar

The stress in the bar is given by (3). The sum term is $\pi/4$ at $t = 0$. Hence the amplitude of the stress is just $\sigma_0 = E\alpha\Delta T$. Assuming a tungsten bar with ρ = 19254 kg m^{-3}, $\alpha = 6\text{x}10^{-6}$ K^{-1}, E = 340 GPa and ΔT = 100 K, gives σ_0 = 204 MPa. For a bar of half-length L = 0.025 m the fundamental periodic time of the oscillations is $t^* = 4$, or $\tau = 4L/c$ = 23.8 ms and the frequency is f_0 = 42 kHz.

It is possible to express the longitudinal motion of the bar from the stress equation (2) using the simple relationship, force equals the rate of change of momentum,

$$F = m\frac{dV}{dt}, \tag{6}$$

where m is the mass. Integration gives the velocity,

$$V = \frac{1}{m}\int F dt \tag{7}$$

and integration once more gives the displacement, w. Consider a slice of the bar of thickness dz at z; the net axial force on the slice is,

$$F(x,t) = A\left[\sigma(x,t) - \sigma(x-dx,t)\right] \tag{8}$$

where A is the area of the slice.

$$V(z,t) = \frac{\int_0^t \left[\sigma(z-dz,t) - \sigma(z,t)\right]dt}{\rho dz} \tag{9}$$

Substituting for the stress (2), and performing a little algebra

$$V(z,t) = \frac{4}{\pi}\frac{E\alpha\Delta T}{\rho dz}\int_0^t \left\{\sum_{n=0}^{\infty}\frac{(-1)^n}{(2n+1)}\left[\cos(2n+1)\frac{\pi}{2L}(z-dz) - \cos(2n+1)\frac{\pi}{2L}z\right]\cos(2n+1)\frac{\pi}{2L}ct\right\}dt$$

$$V(z,t) = \frac{4}{\pi}\frac{E\alpha\Delta T}{\rho dz}\int_0^t \left\{\sum_{n=0}^{\infty}\frac{(-1)^n}{(2n+1)}\left[2\sin(2n+1)\frac{\pi}{2L}\frac{2z-dz}{2}\sin(2n+1)\frac{\pi}{2L}\frac{dz}{2}\right]\cos(2n+1)\frac{\pi}{2L}ct\right\}dt$$

which becomes, as dz approaches zero,

$$V(z,t) = \frac{4}{\pi}\frac{E\alpha\Delta T}{\rho dz}\int_0^t \left\{\sum_{n=0}^{\infty}\frac{(-1)^n}{(2n+1)}\left[(2n+1)\frac{\pi}{2L}\frac{dz}{2}2\sin(2n+1)\frac{\pi}{2L}z\right]\cos(2n+1)\frac{\pi}{2L}ct\right\}dt$$

The integration gives,

$$V(z,t) = \frac{4E\alpha\Delta T}{\pi c\rho}\sum_{n=0}^{\infty}\frac{(-1)^n}{(2n+1)}\sin(2n+1)\frac{\pi z}{2L}\sin(2n+1)\frac{\pi ct}{2L} \tag{10}$$

$$V(z,t) = \frac{4\alpha\Delta T}{\pi\sqrt{c}}\sum_{n=0}^{\infty}\frac{(-1)^n}{(2n+1)}\sin(2n+1)\frac{\pi z}{2L}\sin(2n+1)\frac{\pi ct}{2L} \tag{11}$$

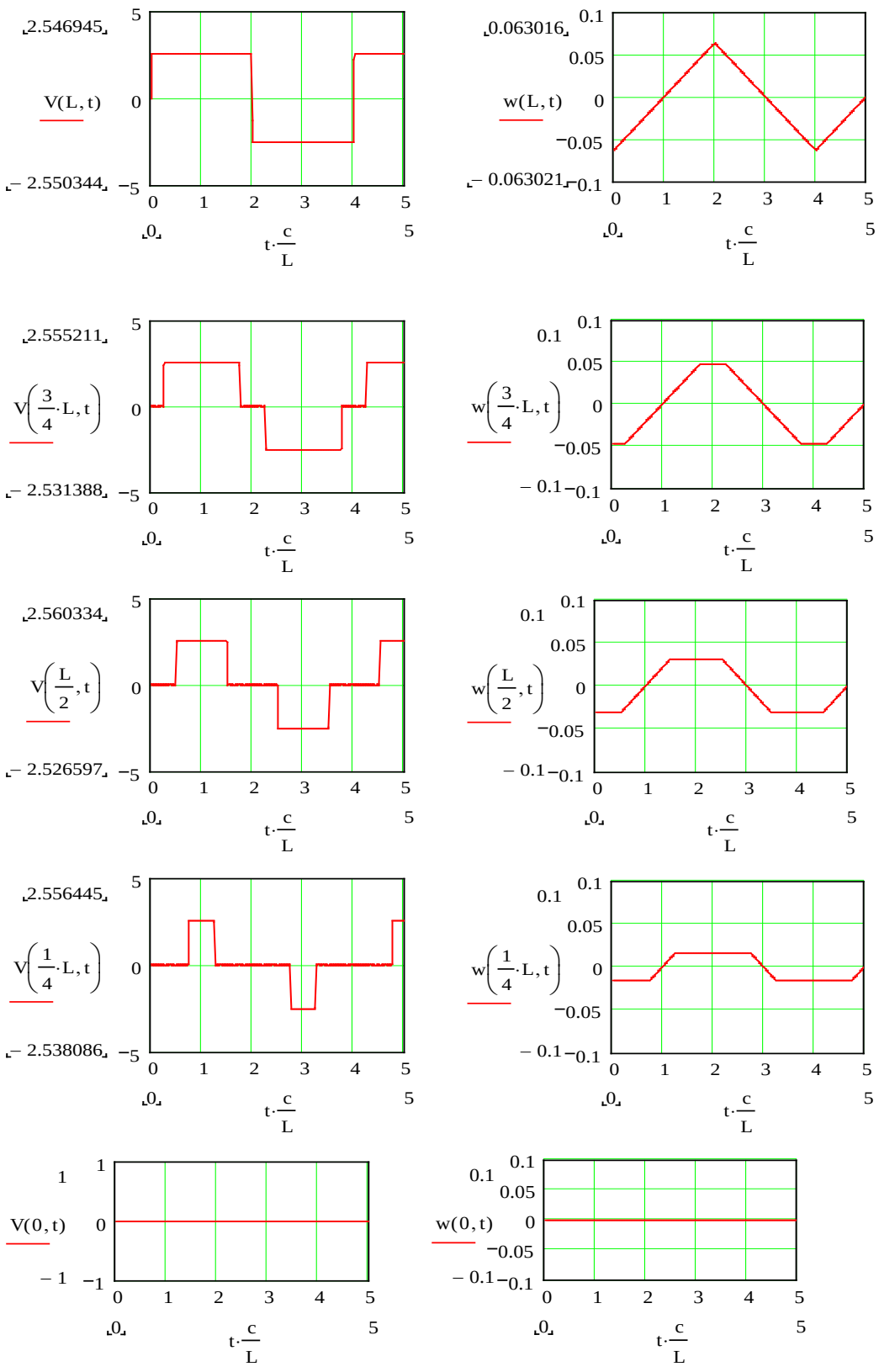

Figure 6. The velocity, $V(z,t)$ and displacement, $w(z,t)$ at different positions along the bar as a function of time, t, using equations (6) and (7).

The displacement, w at any position z along the bar, is found by integrating the velocity,

$$w(z,t) = \frac{8LE\alpha\Delta T}{\pi^2 c^2 \rho} \sum_{n=0}^{\infty} \frac{(-1)^n}{(2n+1)^2} \sin(2n+1)\frac{-\pi z}{2L} \cos(2n+1)\frac{\pi c t}{2L} \tag{12}$$

$$w(z,t) = \frac{8\alpha\Delta T}{\pi^2} \sum_{n=0}^{\infty} \frac{(-1)^n}{(2n+1)^2} \sin(2n+1)\frac{-\pi z}{2L} \cos(2n+1)\frac{\pi c t}{2L} \tag{13}$$

The amplitude of the velocity is $\frac{\alpha\Delta T}{\sqrt{c}} = \frac{E\alpha\Delta T}{c\rho}$ and of the displacement is $\alpha\Delta T$, since the sum terms are $\pi/4$ [5] and $\pi^2/8$ (= G [5]), respectively. Figure 6 shows the axial velocity and displacement as a function of t^* at different positions along the length of the bar.

2.3 Strain

The strain is given by [1],

$$\varepsilon(z,t) = \frac{\sigma(z,t)}{E} = \frac{\partial w(z,t)}{\partial z} = \frac{4\alpha\Delta T}{\pi} \sum_{n=0}^{\infty} \frac{(-1)^n}{(2n+1)} \left\{ \cos\left[\frac{(2n+1)\pi}{2L} z \right] \cos\left[\frac{(2n+1)\pi}{2L} ct \right] \right\} \tag{14}$$

The strain as a function of time at different axial positions along the length of the bar behaves as the stress, as shown in Figure 3. The sum term is $\pi/4$, so the strain amplitude is $\alpha\Delta T$. Figure 7 shows the calculated solution to (14) and the stress for comparison.

2.4 Strain Rate

The strain rate is defined as,

$$\dot{\varepsilon}(z,t) = \frac{\partial \varepsilon(z,t)}{\partial t} \tag{15}$$

which can be expressed as,

$$\dot{\varepsilon}(z,t) = \frac{1}{E}\frac{\partial \sigma(z,t)}{\partial t} = \frac{\partial\left(\frac{\partial w(z,t)}{\partial z} \right)}{\partial t} = \frac{\partial V(z,t)}{\partial z} \tag{16}$$

In the case considered here of a fast pulse of energy entering the bar, the axial strain rate is,

$$\dot{\varepsilon}(z,t) = \frac{-2c\alpha\Delta T}{LE} \sum_{n=0}^{\infty} (-1)^n \cos\left[(2n+1)\frac{\pi z}{2L} \right] \sin\left[(2n+1)\frac{\pi c t}{2L} \right] \tag{17}$$

The strain rate is zero everywhere except where the stress changes – the rising and falling edges of the square wave - at which point the strain rate is plus or minus infinity. Figure 8 illustrates this schematically. The strain rate has a fundamental frequency of f_0 = c/4L.

Note that for quasi static cases where the bar does not suffer from vibrations; the stress and strain are not functions of z, but the velocity varies linearly with z.

$$\dot{\varepsilon}(t) = \frac{\partial \varepsilon(t)}{\partial t} = \frac{1}{z}\frac{\partial w(z,t)}{\partial t} = \frac{1}{z} V(z,t) \tag{18}$$

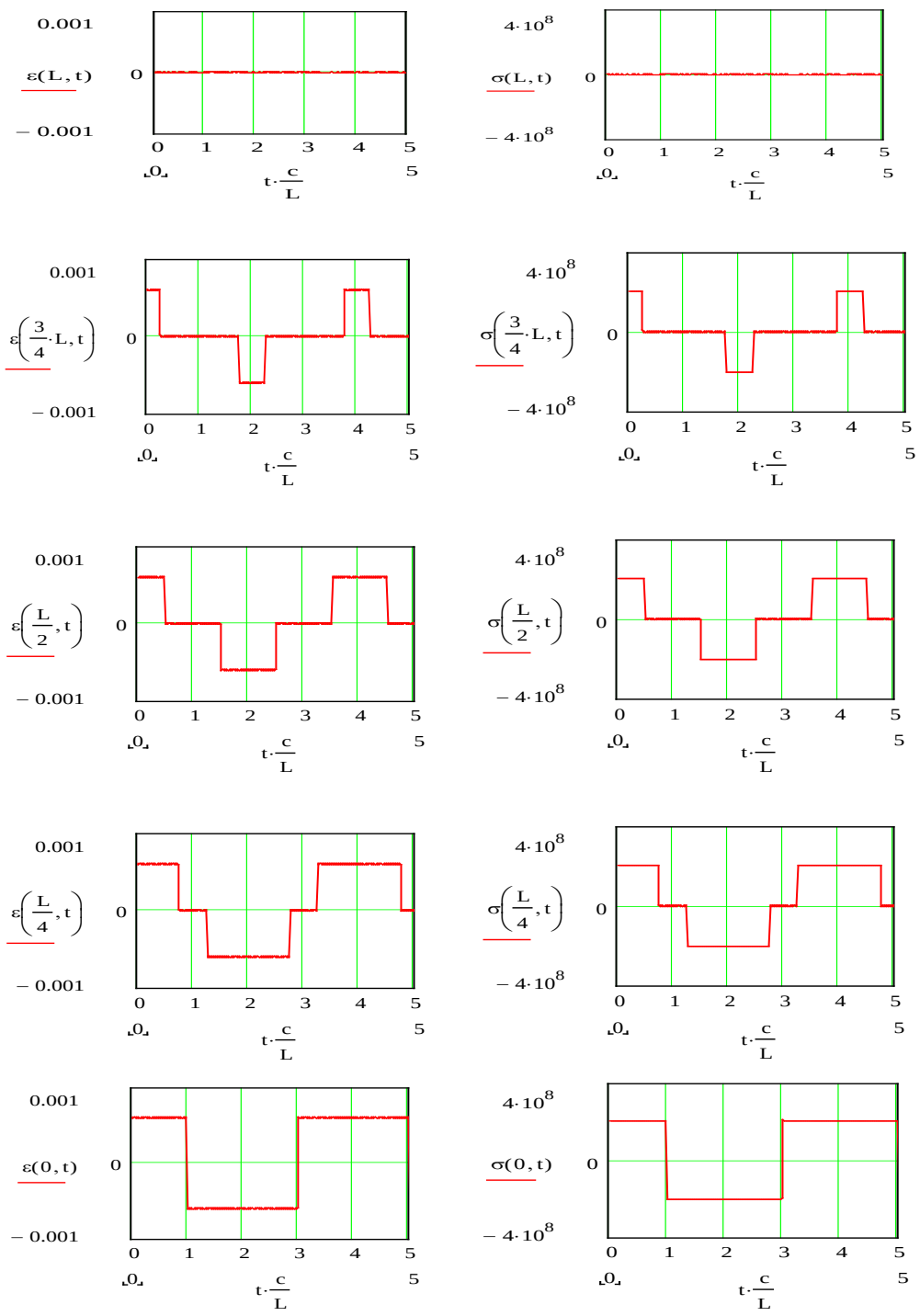

Figure 7. Axial strain and stress as a function of time, *t**, at different positions along the bar.

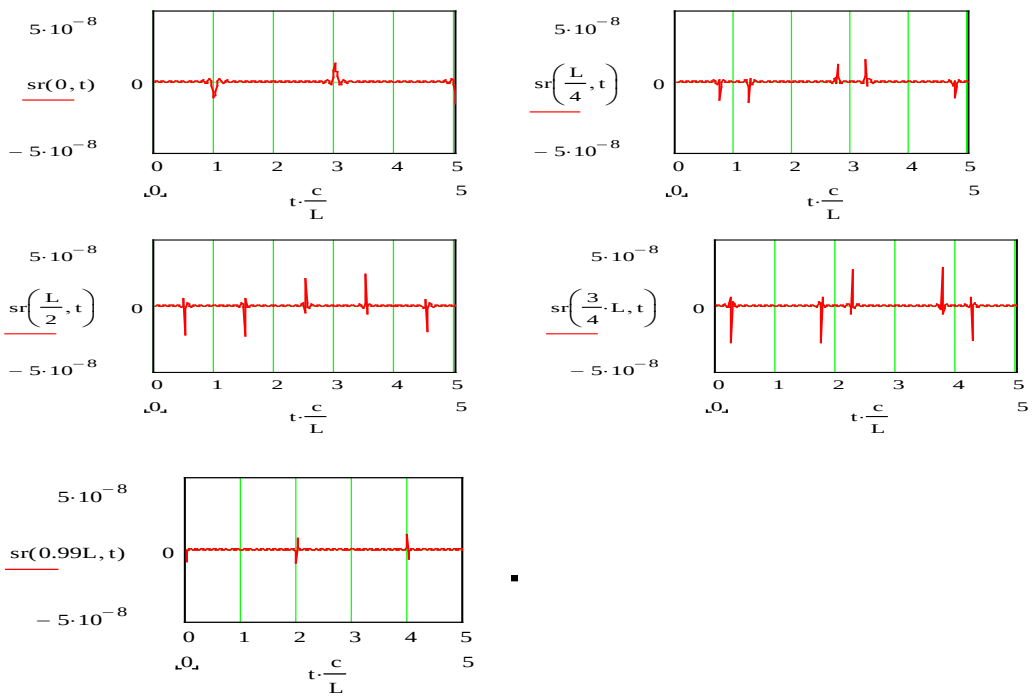

Figure 8. Schematic diagrams showing when in time, t^*, the strain rate, sr(z,t), becomes infinite at different axial positions along the bar. The vertical lines indicate the times at which the strain rate is non zero and give no indication of their magnitude (the rate is $+\infty$ or $-\infty$ at these instants in time).

2.5 Strength and Strain Rate

The strength of a material is dependant on the strain rate [5]. The strain rate varies with time from $+\infty$ to $-\infty$, but is zero for most of the time. So what is the appropriate strain rate when assessing the strength?

3. Axial Stress, Strain and Motion with a Finite Pulse

3.1 The Quasi-Static Case

Now consider heat density entering the bar uniformly at a rate p over a time t_0 which is much longer than the period, τ, of the longitudinal natural resonant frequency, $f_0 = c/4L$, of the bar. This is a quasi-static situation. Figure 9 shows schematically the rate of energy density, p, entering the bar with time and the consequent longitudinal thermal expansion, λ, of the bar. The temperature rise is the same shape as the expansion (for constant α).

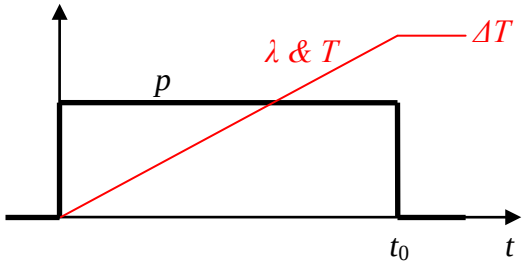

Figure 9. Energy pulse into the bar, thermal expansion and temperature as a function of time.

The integrated heat into the bar is,

$$Q = pt_0 \tag{19}$$

and the temperature rise is,

$$\Delta T(t) = \int_0^{t_0} \frac{p(t)}{\rho C} dt = \frac{pt_0}{\rho C} \tag{20}$$

where C is the specific heat. Each end of the bar expands by,

$$\lambda(t) = \alpha L \int_0^{\theta} \Delta T(t) dt = \frac{\alpha L p t_0}{\rho C} \tag{21}$$

The temperature and expansion rise linearly with the constant input of heat during the length of the pulse. The velocity of the end of the bar increases linearly with time during the pulse,

$$V(t) = \alpha L \Delta T(t) = \frac{\alpha L p}{\rho C} t \tag{22}$$

and falls to zero at the end of the pulse.

3.2 The Intermediate Case

For the case where the energy pulse is reasonably short but of finite duration, t_0, the stress during the pulse is given by [3,4]. Consider the case of a square wave of energy of length t_0 entering the bar so that the temperature rises linearly with time as shown in Figure 9, the stress in the bar behaves similarly to the instantaneous pulse case (Figure 2) but produces sloping rises to the “squares".

The equation for the stress is [4],

$$\sigma_i(z,t) = \frac{8LE\alpha\Delta T}{\pi^2 c t_0} \sum_{n=0}^{\infty} \frac{(-1)^n}{(2n+1)^2} \sin(2n+1)\frac{\pi c}{2L} t \cos(2n+1)\frac{\pi z}{2L}, \qquad \text{for } 0 \le t \le t_0$$

$$\sigma_f(z,t) = \frac{8LE\alpha\Delta T}{\pi^2 c t_0} \sum_{n=0}^{\infty} \frac{(-1)^n}{(2n+1)^2} \left[\sin(2n+1)\frac{\pi c}{2L} t - \sin(2n+1)\frac{\pi c}{2L}(t - t_0) \right] \cos(2n+1)\frac{\pi z}{2L}, \quad \text{for } t \le t_0 \tag{23}$$

Figure 10 shows the axial stress in the bar as a function of the length at different times, t^*, in units of L/c. The length of the pulse is chosen as $t_0 = L/4c$ for convenient illustration purposes. The stress builds up over the time t_0 and then falls to zero as the triangular relaxation wave travels from the ends of the rod. Figure 11 shows the stress as a function of time at different positions along the bar.

The strain waveforms are similar to Figure 11, since $\varepsilon_z = \sigma_z/E$. The peak strain amplitude is

$$\varepsilon_z = \alpha \Delta T \tag{24}$$

The strain rate varies with z and is either 0, or finite at various points along the bar depending on the time, when the strain rate is,

$$\dot{\varepsilon}_z = \frac{\varepsilon_z}{t_0}, \text{ at all values of } z \text{, except at, } -ct_0 > z < ct_0 \tag{25}$$

At values of z between $+ ct_0$ and $-ct_0$, the strain rate increases until it reaches a maximum of,

$$\dot{\varepsilon}_z = \frac{2\varepsilon_z}{t_0}, \text{ at } z = 0, \text{ except at, } t = 0 \text{ to } t = t_0. \tag{26}$$

However, the strain is expected to be zero at $z = 0$, but close to $z = 0$ the strain rate is calculated to be $2\varepsilon_z/t_0$.

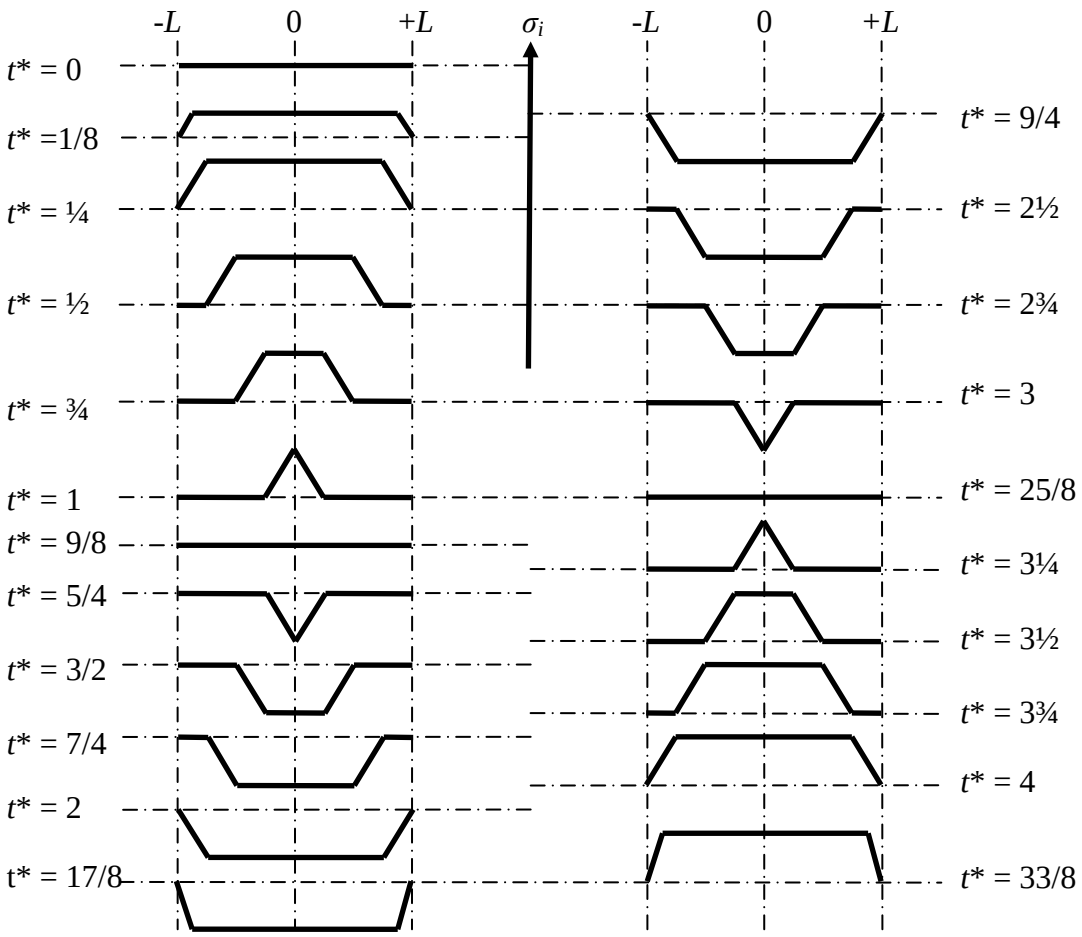

Figure 10. Axial stress, σ_i, along the bar at different times, t^*, with a linear rise of the temperature in time $t_0 = L/4c$.

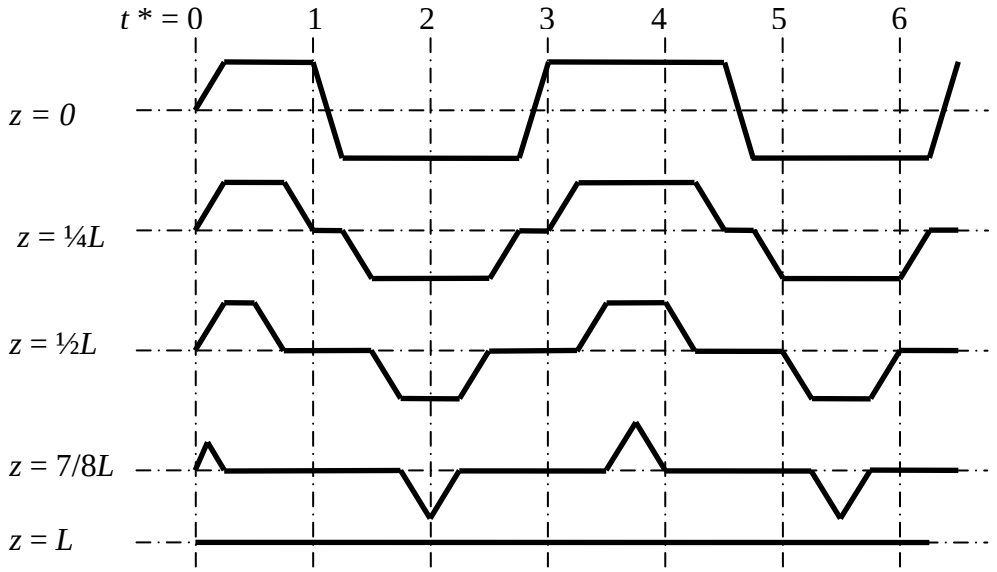

Figure 11. Stress as a function of time, t^*, at different positions along the bar. The temperature rise time is, $t_0 = L/4c$.

For $0 \le t \le t_0$, the velocity, shown in Figure 12, is given by,

$$V_i(z,t) = \frac{8LE\alpha\Delta T}{\pi^2 t_0 c^2 \rho} \sum_{n=0}^{\infty} \frac{(-1)^n}{(2n+1)^2} \left[1 - \cos(2n+1)\frac{\pi}{2L}ct\right] \sin(2n+1)\frac{\pi}{2L}z \qquad (27)$$

Integrating V_i with respect to t gives the displacement w, which is displayed in Figure 13.

$$w_i(z,t) = \frac{8LE\alpha\Delta T}{\pi^2 t_0 c^2 \rho} \sum_{n=0}^{\infty} \frac{(-1)^n}{(2n+1)^2} \left[t - \frac{\sin(2n+1)\frac{\pi}{2L}ct}{(2n+1)\frac{\pi}{2L}c}\right] \sin(2n+1)\frac{\pi}{2L}z \qquad (28)$$

The velocity and displacement are zero for $z \le ¾\ L$. The velocity increases linearly with time, but the displacement w does not; this also applies after $t = t_0$.

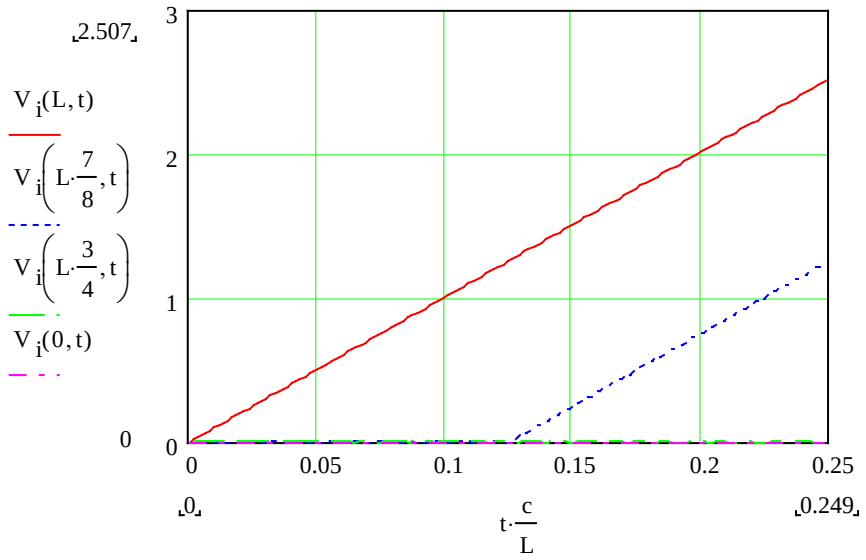

Figure 12. The axial velocity at various points along the bar in the time period $0 \le t \le t_0$, versus t^*; $t_0 = L/4c$.

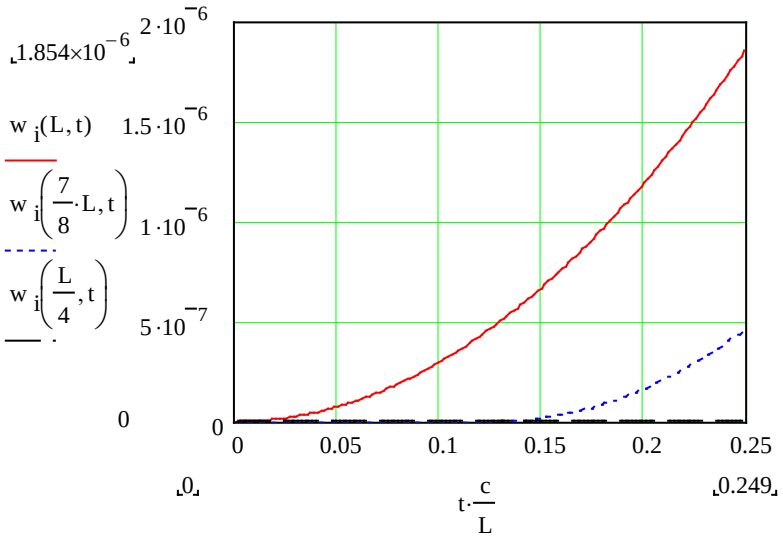

Figure 13. The axial displacement at various points along the bar in the time period $0 \le t \le t_0$, versus t^*; $t_0 = L/4c$.

For $t > t_0$, the velocity, shown in Figure 14, is given by,

$$V_f(z,t) = \frac{8LE\alpha\Delta T}{\pi^2 t_0 c^2 \rho}\sum_{n=0}^{\infty}\frac{(-1)^n}{(2n+1)^2}\sin\left[(2n+1)\frac{\pi}{2L}z\right]\left\{\begin{matrix}1+\cos\left[(2n+1)\frac{\pi}{2L}c(t-t_0)\right]- \\ \cos\left[(2n+1)\frac{\pi}{2L}ct\right]-\cos\left[(2n+1)\frac{\pi}{2L}ct_0\right]\end{matrix}\right\}+V_i(z,t_0) \qquad (29)$$

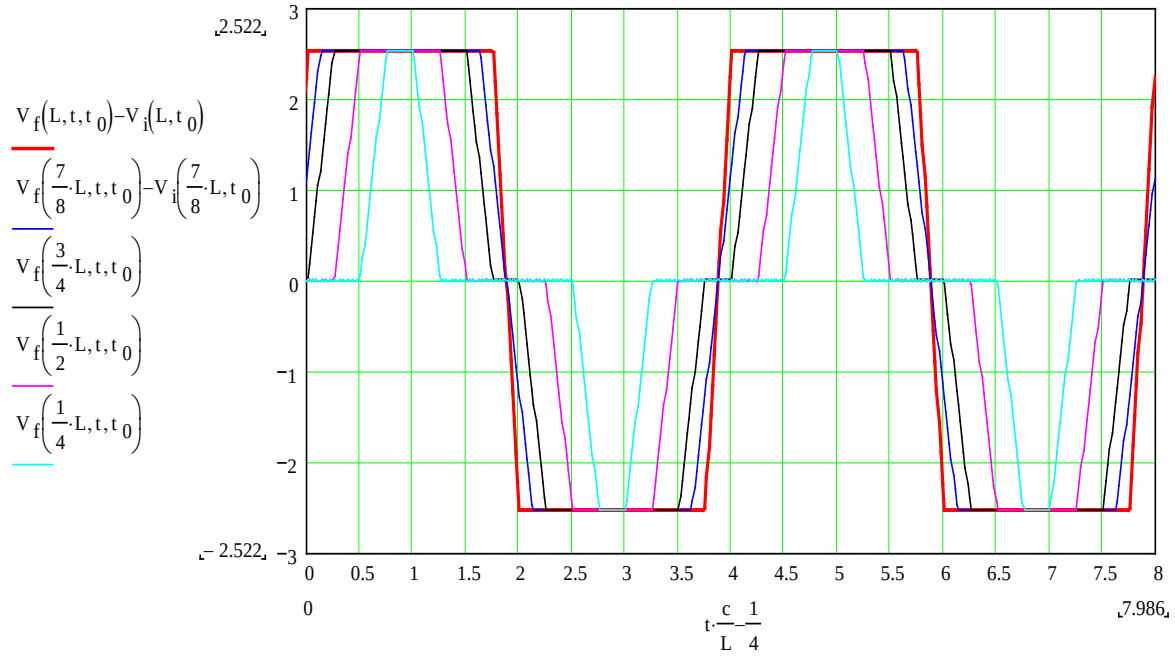

Figure 14. The axial velocity at various points along the bar in the time period $t > t_0$, versus t^*. The time axis starts a $t = t_0 = L/4c$.

The displacement is the integral of the velocity, which for $t > t_0$ is,

$$w_f(z,t) = \frac{8LE\alpha\Delta T}{\pi^2 t_0 c^2 \rho}\sum_{n=0}^{\infty}\frac{(-1)^n}{(2n+1)^2}\sin\left[(2n+1)\frac{\pi}{2L}z\right]\times$$

$$\left\{(t-t_0)\left[1-\cos(2n+1)\frac{\pi c}{2L}t_0\right]\frac{\left[\sin(2n+1)\frac{\pi c}{2L}(t-t_0)-\sin(2n+1)\frac{\pi c}{2L}t+\sin(2n+1)\frac{\pi c}{2L}t_0\right]}{(2n+1)\frac{\pi c}{2L}}\right\} \qquad (30)$$

Figure 15 shows w_f as a function of time, $t \geq t_0$, with $t_0 = ¼L/c$, at various positions along the bar, $z \leq ¾L$. The maximum excursion from zero is $2z\alpha\Delta T$, which gives $2L\alpha\Delta T$ at the end of the bar, that is, twice the thermal expansion. Notice that the shape of the displacement curves is similar to the case of instant increase in temperature, but with a linear ramp during the period of constant velocity and curves where the velocity ramps up and down.

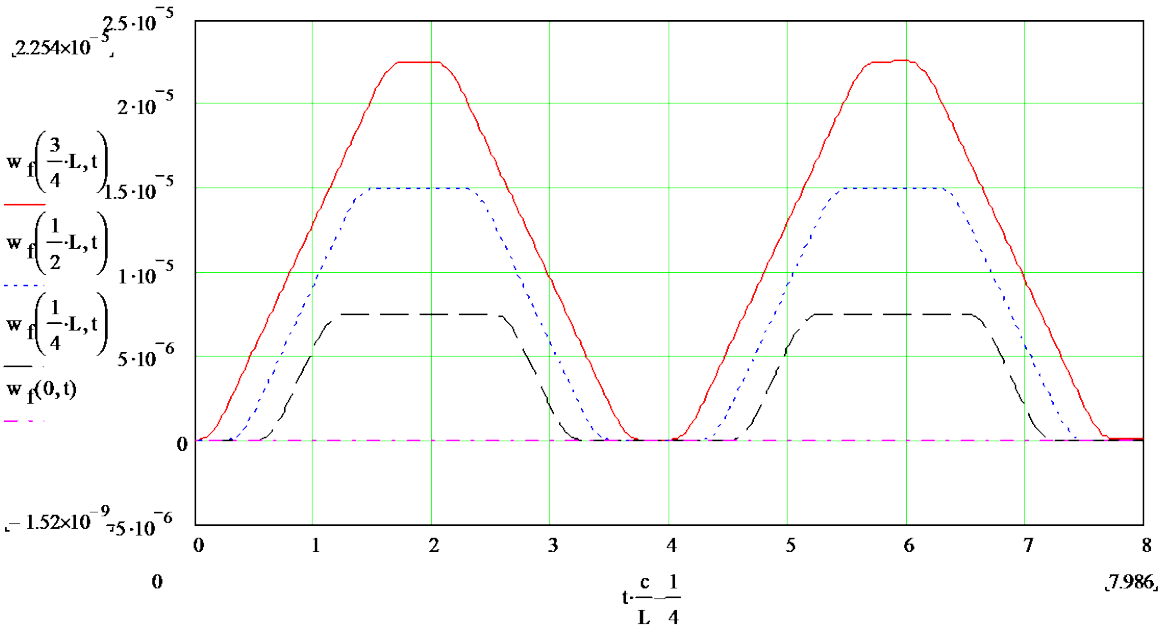

Figure 15. Axial displacement at various points along the bar as a function of t^* from $t = t_0 = c/4L$. For $z > ¾\ L$ the initial velocity and displacement at t_0 must be taken into account.

4. Radial Stress, Strain and Motion

The radial stress of a free bar is not solvable analytically [4]. However, the radial frequency of oscillation is given approximately by Airey [8] for a long thin bar and by Lin [9] and Abe, Tanaka and Uo [10] for a bar of any ratio of length to diameter. Observation by laser optical interferometry of the radial surface vibrations of thin wires of tungsten and tantalum shows that the radial velocity is sinusoidal with time. The frequency agrees very well with the formula of Airey. The longitudinal velocity waveform agrees with the analytical results. In these tests the wire is heated by an electrical current pulse, shown in Figure 16.

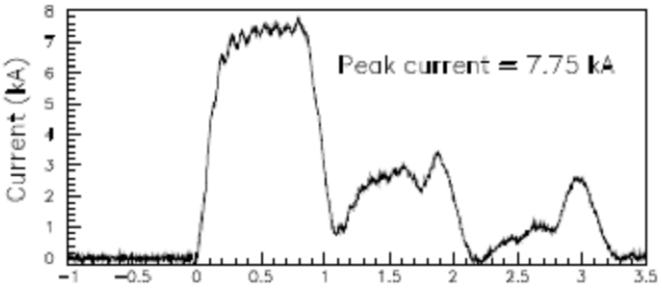

Figure 16. The measured current pulse. The x-axis is in units of μs.

4.1 Radial Motion with Slow Pulse Heating.

The wire has dimensions as given in Section 2.2. The pulse is about ten times longer than the radial periodic time [8] (frequency ~7 MHz), hence the bar sees an almost quasi-static application of heat during the current pulse in the radial dimension. The radial vibrations

excited by the pulse are ignored. The current pulse shown in Figure 16 can be represented with good accuracy by the sum of two exponential terms with different time constants, τ_1, τ_2, and amplitudes, I_1, I_2,

$$I(t) = I_0\left[I_1(1-\exp-\frac{t}{\tau_1}) + I_2(1-\exp-\frac{t}{\tau_2}) \right] \tag{31}$$

With the correct choice of the parameters in equation (31), this replicates the current pulse (see Figure 16) applied to the tungsten wires in the measurements of strength, Young's modulus of elasticity and lifetime at high stress, temperature and strain rate. The subsequent smaller pulses in Figure 16 are ignored. The pulse lasts for ~1 μs and is shown in Figure 17.

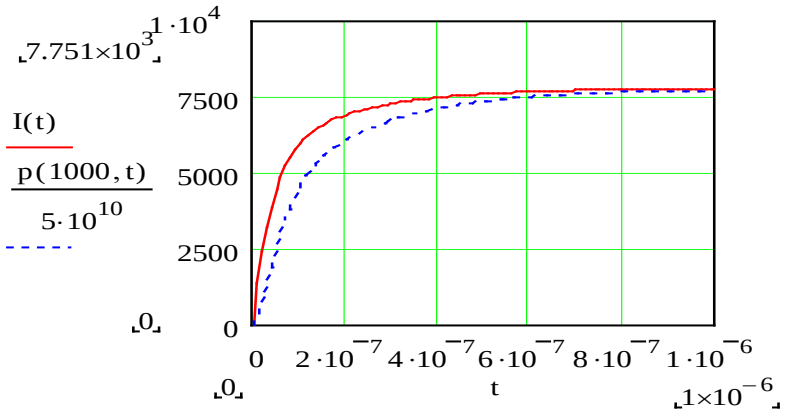

Figure 17. The current pulse in the wire. The peak current is 7750 A. The power density versus time is also shown.

The power generated as a function of time per unit volume is,

$$p(T,t) = I(t)^2 \rho(T) \frac{1}{(\pi a^2)^2} \tag{32}$$

where the electrical resistivity, $\rho(T)$, is a function of the absolute temperature. It will be seen that the power density is very high ~10^{14} W m^{-3} and has been reduced by 5x10^{10} in the figure to show that the slow rise in current after 100 ns still produces an appreciable rise in power density due to the square of the current. If $C_p(T)$ is the specific heat of the tungsten as a function of temperature then the temperature rise with time is,

$$T(T,t) = \int \frac{p(T,t)}{dC_p(T)} dt \tag{33}$$

where the limits of integration are t = 0 and t = 10^{-6} s and $r(T)$ is the change in radius with temperature, then the velocity of the surface of the wire is given by,

$$V(T,r) = \frac{dT(T,t)}{dt}\frac{dr(T)}{dT} \tag{34}$$

Figure 18 shows the calculated surface velocity at various peak temperatures and Figure 19 shows the measured values at similar temperatures. The calculated curves are generally slightly lower than the measured ones (ignoring the radial resonant vibrations).

The surface strain rate is,

$$\dot{\varepsilon} = \frac{V(T,a)}{a} = \frac{\alpha \Delta T}{t_0} \tag{35}$$

where t_0 is the length of the pulse. In the tests of the 0.5 mm diameter tungsten wires, the strain rate is typically 1000 s^{-1}.

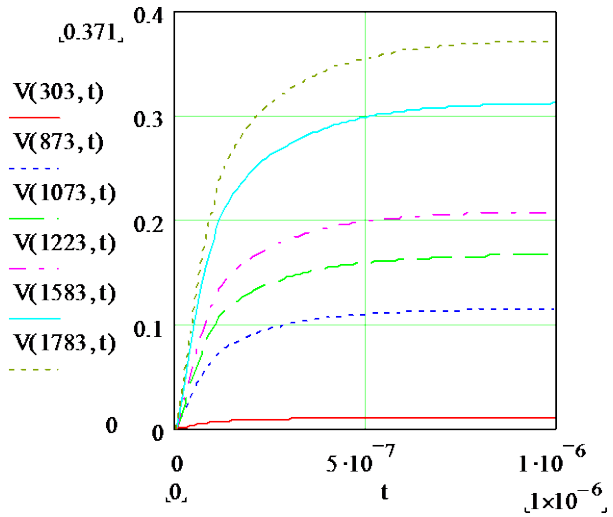

Figure 18. The surface radial velocity of a 0.5 mm diameter tungsten wire at various initial temperatures (in Kelvin).

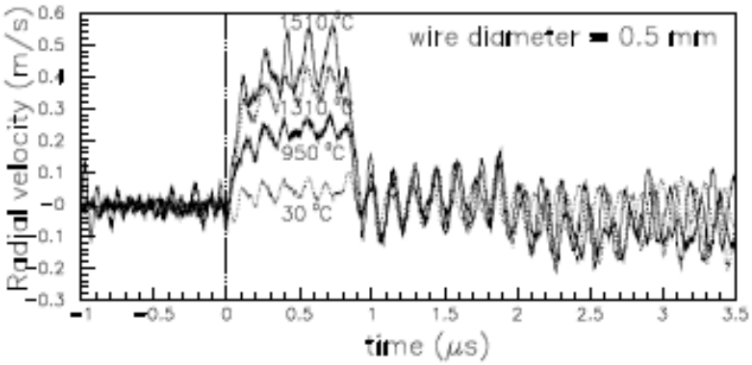

Figure 19. The measured surface radial velocities at several initial temperatures (in °C).

4.2 The Radial Resonant Vibrations.

It will be seen, from Figure 19, that the radial amplitudes of the resonant oscillations are about one tenth of the displacement due to the quasi-static temperature rise, except at low currents during the pulse. After the current pulse the amplitudes of the oscillations are always about the same whatever the current pulse.

The thermal expansion of the wire continues throughout the current pulse and any forces due to this therefore cover many periods of the radial resonant oscillation. The result is that the signal alternately adds or opposes the initial "kick" that starts the radial resonance. As a result the amplitude of the radial motion at the surface is not $\alpha\Delta Ta$, but is reduced approximately to the kick that corresponds to the temperature rise in ¼ to ½ the resonant period. In the case studied here this corresponds to about 1/10 of the quasi-static temperature rise at the end of the pulse.

In addition to the stress applied by the increase in temperature, there is a radial force due to the magnetic field produced by the wire, given by the time dependent vector relation [6],

$$\rho \frac{dV_r}{dt} = -\nabla p + \mathbf{j} \times \mathbf{B} \tag{36}$$

where V_r is the radial velocity, **j** the current density, **B** the magnetic induction and p the pressure. For a steady current, the "pinch" pressure on the wire as a function of radius is,

$$p_r(t) = \frac{\mu_0}{4\pi^2 a^2} I(t)^2 \left(1 - \frac{r^2}{a^2}\right) \tag{37}$$

where $I(t)$ is the current, assumed to be uniform throughout the wire and μ_0 is the permeability of free space; the external pressure on the wire is assumed to be zero. The maximum pressure is at the centre of the wire; the pressure on the surface is zero. In the case of a peak current of 7.75 kA the maximum pressure is nearly 31 MPa, see Figure 20.

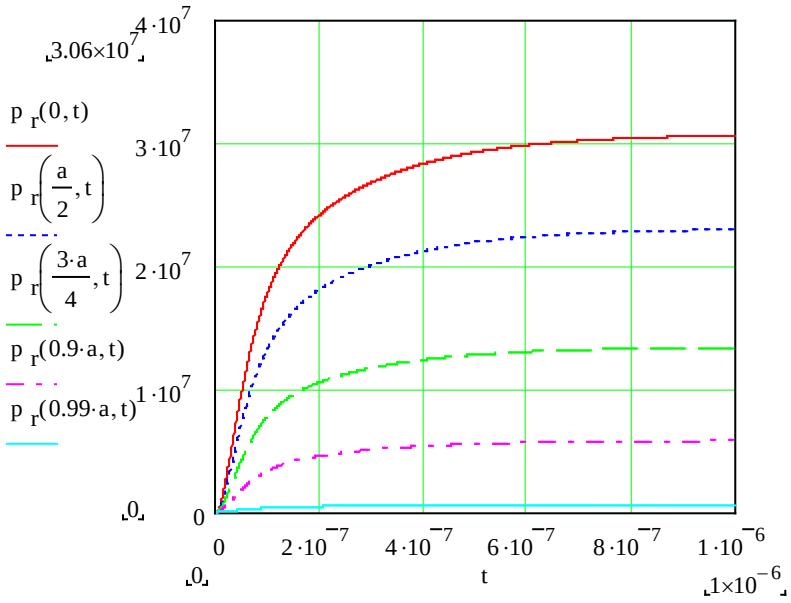

Figure 20. The radial pressure (Pa) at different radii within a 0.25 mm radius tungsten wire as a function of time with the current pulse shown in Figure 10 of 7.75 kA peak.

Of course the current pulse initially flows in the surface of the wire and gradually diffuses in towards the centre. The large stress generated by the self magnetic field can certainly initiate the radial vibrations. However the magnetic forces are opposed to the initially thermal forces, when the temperature is increasing, and relax when the current pulse falls. The change in resistivity and thermal expansion coefficient with temperature of tungsten is relatively high, so both the power dissipated in the wire and the thermal expansion increase significantly with the temperature. In contrast, the magnetic pressure is independent of the wire temperature. Hence, at low temperatures and low currents, a small negative velocity in the radial surface motion is observed at the beginning of the pulse, see Figure 19, where the magnetic force is dominant. At higher temperatures where the thermal force is larger, the initial velocity is positive. However, at the end of the pulse the relaxation of the magnetic field gives the rod another radial "kick". As a result of both the magnetic and thermal effects the amplitude of the radial velocity and displacement is roughly constant with current after the current pulse.

The displacement at the surface of the rod can be represented by a simple sinusoid,

$$w(t) = A(1+\sin\omega t)$$

The velocity is then,

$$V(t) = \frac{dw(t)}{dt} = A\omega\cos\omega t \tag{38}$$

where A is the amplitude of the oscillation at the surface and ω the angular frequency.

The strain rate is,

$$\dot{\varepsilon}(t) = \frac{A\omega}{a}\cos\omega t = \frac{V(t)}{a} \tag{39}$$

The amplitude of the strain rate is just $A\omega/a$, which can be expressed as,

$$\frac{A\omega}{a} = \frac{a\alpha\Delta T}{a}\frac{\tau}{4t_0}\omega = \alpha\Delta T\frac{2\pi}{4t_0} = \frac{\pi}{2t_0}\alpha\Delta T \approx \frac{\alpha\Delta T}{t_0} \tag{40}$$

where τ is the periodic time of the oscillation and t_0 is the duration of the current pulse. This is the same as the longitudinal value (section 3.2 equation (25)) and the slow radial value (section 4.1, equation (35)). Note that if the time, $\tau/4$, taken for the assumed period of time to initiate the resonant oscillation had been chosen as $\tau/2\pi$, the equation (40) would have been exact. Since the strain rate must approach $\alpha\Delta T/t_0$ as the pulse length t_0 becomes much shorter than the period of oscillation, τ, it is reasonable to infer that the amplitude of the strain rate is reduced by the ratio $\tau/2\pi t_0$, rather than $\tau/4t_0$. Hence, (40) becomes exactly, $\dot{\varepsilon} = \alpha\Delta T/t_0$.

5. Strain Rate

Given that the strain rate can be expressed generally throughout the bar as,

$$\dot{\varepsilon} = \frac{\alpha\Delta T}{t_0} \tag{41}$$

Typically in the full size tungsten target (2 cm diameter, 20 cm long) the mean temperature will be ~1500 K with ΔT ~30 K. The strain rate with a 2 ns long proton beam pulse is ~2000 s^{-1}.

It is possible to express (41) in terms of the energy density in the bar, q,

$$\dot{\varepsilon}(T) = \frac{\alpha(T)}{C(T)}\frac{q}{\rho t_0} \tag{42}$$

Assuming the energy deposited is inversely proportional to the square of the radius of the bar,

$$\dot{\varepsilon}(a,T) = \frac{\alpha(T)q_0}{C(T)\rho t_0 a^2} \tag{43}$$

where q_0 is the energy in a 1 m radius bar, then the strain rate will decrease as the square of the radius. Figure 21 shows the variation of as a function of temperature. At the proposed operating temperature of the neutrino factory target of ~1500 K, $\alpha(T)/C(T) = 3.45\text{x}10^{-8}$ J kg^{-1} T^{-1}.The power absorbed by the target is ~700 kW or 14000 J per pulse giving an average energy density in a 20 cm long target of, $q_0 = 14000/0.2\pi = 2230$ J m^{-3}. With the density of tungsten, $\rho = 19254$ kg m^{-3}, this gives for the average strain rate,

$$\dot{\varepsilon} = \frac{4\cdot 10^{-8}}{t_0 a^2} \tag{44}$$

For a proton beam pulse of length, t_0 = 2x10^{-9} s and a target of radius, a = 0.01 m, the average strain rate is 2000 s^{-1}. The peak energy density is up to about twice the average, doubling the strain rate. Figure 22 shows the average strain rate as a function of radius for target radii of 2 to 20 mm, 20 cm long. The use of several nanosecond long micro-pulses per macro-pulse reduces the stress so that the peak value is near the average.

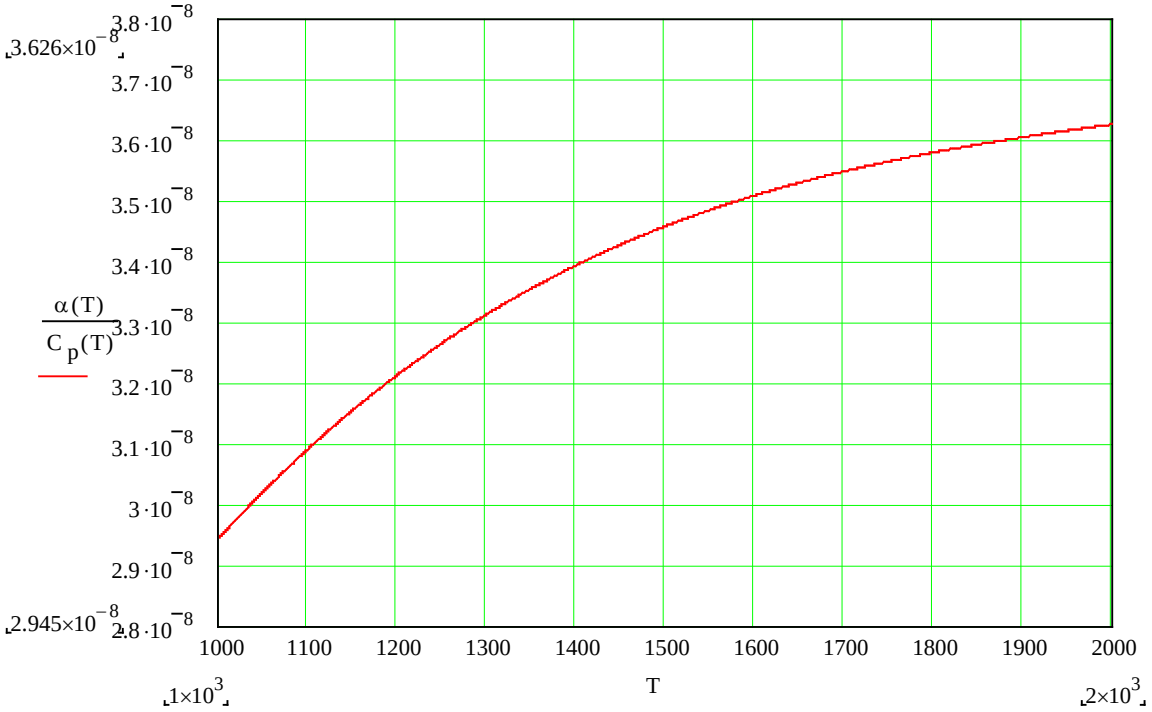

Figure 21. Plot of $\alpha(T)/C(T)$ as a function of temperature (K).

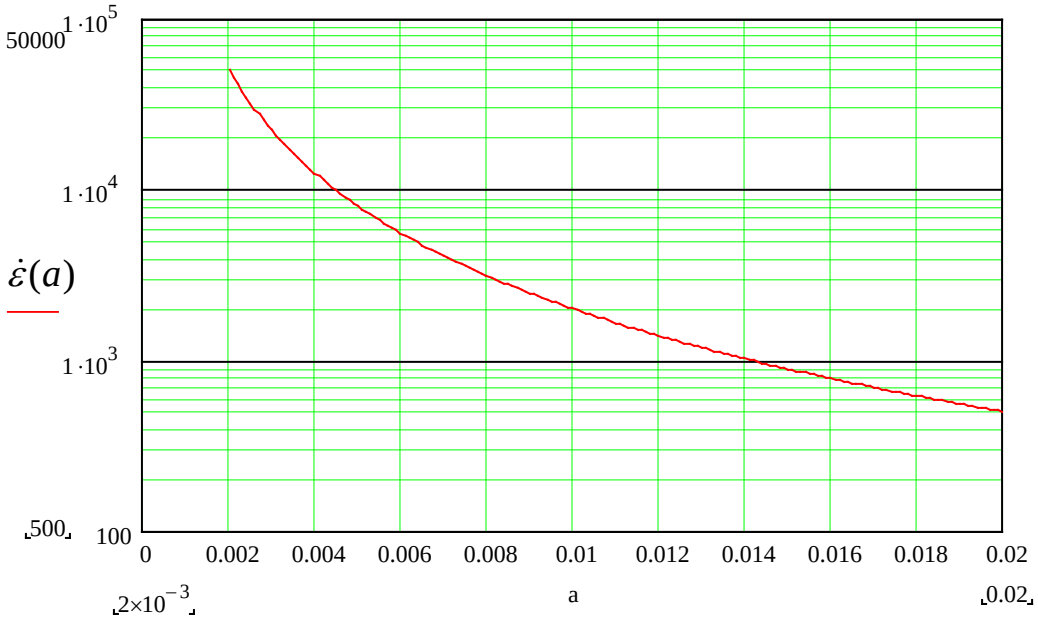

Figure 22. Strain rate (s^{-1}), on a log scale, versus target radius (m) for a 20 cm long tungsten target, bombarded by a 4 MW proton beam (700 kW absorbed in the target at 50 Hz pulse repetition rate, 2 ns long pulse).

6. Summary of Effects

The amplitude of the displacement excitation is approximately given by $\alpha\delta TL$ (ignoring the magnetic force) in the axial direction and $\alpha\delta Ta$ in the radial, where δT is the temperature rise in $1/2\pi$ of the periodic time of the relevant oscillation period. In the extremes of very slow temperature rises the amplitude of the resonant vibration approaches zero (the quasi-static case) and when the pulse of the temperature rise is equal to or shorter than $1/2\pi$ of the periodic time all the energy of the pulse goes into the excitation.

Hence, the waveform of the observed displacement will be a combination of the waveform of the energy from the current pulse and, depending on the duration of the current pulse relative to the resonant period, some proportion of this amplitude at the resonant frequency. Of course the effect of the magnetic force must also be taken into account along with the thermal expansion.

In addition, the longitudinal stress is to be seen in the radial motion through Poisson's coefficient and likewise the radial stress is seen in the longitudinal.

The strain rate in radial and longitudinal directions is the same value including the slow and fast components of motion; but there would appear to be an anomaly at the centre of the bar, $z = 0$, where the longitudinal strain rate is doubled. It is not known (due to the lack of an analytical result) if there is a similar effect radially near the axis of the bar.

References

[1] S. P. Timoshenko and J. N. Goodier, Theory of Elasticity, McGraw-Hill, 1970.

[2] A. E. H. Love, A Treatise on the Mathematical Theory of Elasticity, Cambridge University Press, 1906.

[3] H. Bargmann, Dynamic Response of External Targets under Thermal Shock, CERN Report Lab. II/BT/Int./73-3, 1973.

[4] P. Sievers, Elastic Stress Waves in Matter due to Rapid Heating by an Intense High-Energy Particle Beam. CERN Report, Lab. II/BT/74-2, 1974.

[5] H. B. Dwight, Tables of Integrals and Other Mathematical Data, McMillan, New York, 1957.

[6] R. W. Armstrong and S. M. Walley, Int. Metals. Rev, 53 (2008) 105.

[7] P. Krehl, J. Phys. D: Appl.Phys., 6 (1973) 2187.

[8] Airey J. R. Airey, Archiv der Mathematik und Physik. Series 3, Volume 20 (1913) 289.

[9] S.-Y. Lin, Journal of Sound and Vibration, 185 (1995) 193.

[10] K. Abe, T. Tanaka and K. Uo, Journal of the Denki Hyoron (Electrical Review, Japan), **39**, no 12 (1951) p. 2.

[11] K. Abe, T. Tanaka and K. Uo, Bulletin of the Institute for Chemical Research, Kyoto University, 29: p 71-72, (1952). http://hdl.handle.net/2433/74436

[12] K. Abe, T. Tanaka and K. Uo, Bulletin of the Institute for Chemical Research, Kyoto University, 31(1), p 51-52, (1953). http://hdl.handle.net/2433/75271

[13] K. Abe, T. Tanaka and K. Uo, Bulletin of the Institute for Chemical Research, Kyoto University, 31(3): p 208-211, (1953). http://hdl.handle.net/2433/75327